The photoionization dynamics of the three structural isomers of dichloroethene

Parkes, Michael; Ali, S; Howle, CR; Tuckett, Richard; Malins, AER

DOI:
10.1080/00268970600976055

The photoionisation dynamics of the three structural isomers of dichloroethene

M.A. Parkes,* S. Ali, C.R. Howle and R.P. Tuckett

Mol. Phys., (2007) **105**, 907-916

DOI : 10.1080/00268970600976055

Revised version following comments of referee, 21.8.06 Reference MP6.7.500JB

The photoionisation dynamics of the three structural isomers of dichloroethene

M. A. Parkes,[a] S. Ali,[a] C. R. Howle[*, a] R. P. Tuckett [#, a] and A.E.R. Malins [b]

[a] *School of Chemistry, University of Birmingham, Edgbaston, Birmingham, B15 2TT, U.K.*
[b] *CCLRC Daresbury Laboratory, Daresbury, Warrington,, WA4 4AD, U.K.*

Number of pages : 14 (excluding figure captions and figures)
Number of tables : 3
Number of figures : 4

[*] Current address : Chemical Sciences Division, Lawrence Berkeley National Laboratory, Berkeley CA 94720, USA

[#] Author for correspondence : (fax) +44 121 414 4403 (email) r.p.tuckett@bham.ac.uk

In honour of Professor John Brown's 65th birthday festschrift

---

Using tunable vacuum-UV radiation from a synchrotron, the threshold photoelectron spectrum, threshold photoelectron photoion coincidence spectrum and ion breakdown diagram of the 1,1, *cis*-1,2 and *trans*-1,2 isomers of $C_2H_2Cl_2$ have been recorded in the range 9–23 eV. The energies of the peaks in the threshold photoelectron spectrum are in good agreement with outer-valence Greens function caculations. The major difference between the isomers, both predicted and observed experimentally is that the $\widetilde{F}$ and $\widetilde{G}$ states of $C_2H_2Cl_2^+$ are approximately degenerate for 1,1 and *trans*-1,2, but well separated for the *cis*-1,2 isomer. The ground and low-lying valence states of $C_2H_2Cl_2^+$ are bound, with higher-lying states dissociating to $C_2H_2Cl^+$ or $C_2H_2^+$. The translational kinetic energy release into $C_2H_2Cl^+ + Cl$ is determined as a function of energy. Isolated-state behaviour for the low-lying electronic states of $C_2H_2Cl_2^+$ becomes more statistical as the energy increases.

1. Introduction

It is of fundamental interest to study the effect of structural isomerisation on both the reactivity and dynamics of molecules. Dichloroethene, $C_2H_2Cl_2$, is an environmental pollutant and a potential human carcinogen [1]. It exists in three isomeric forms, 1,1-, *cis*-1,2- and *trans*-1,2-, and we reported recently the rate coefficients and product branching ratios for the gas-phase reactions of these three isomers of $C_2H_2Cl_2$ with a range of small cations [2]. Large isotope effects were observed for the reactions of CF_3^+, CF^+ and H_3O^+, cations with recombination energy (RE) less than the ionisation energy (IE) of $C_2H_2Cl_2$, but small isotope effects were also observed for ions with RE values above the IE ($C_2H_2Cl_2$). We also compared the yields for each reaction to the ion yields from a photon-induced threshold photoelectron photoion coincidence (TPEPICO) study to determine the importance of long-range charge transfer in such reactions [3,4]. We have previously studied the reactions of these three isomers with small anions [5]. Significant variations between the reactions of the three isomers were observed, but they were different in nature to the isomeric effects observed in the cation study. In this paper we present a more complete account of the TPEPICO results. There have been many previous studies of ionisation of $C_2H_2Cl_2$ at modest resolution, including several He(I) photoelectron studies [6-9], photoionisation [10], electron impact [11] and electron-electron coincidence spectroscopy [12-14]. Higher resolution, laser-induced pulsed field ionisation-photoelectron and mass-analysed threshold ionisation spectra have been reported for the *trans*-1,2 isomer [15,16]. There have been no studies, however, which combine the measurement of both photoelectrons and photoions under coincidence conditions. The main aim of this study was to see whether the three isomers of $C_2H_2Cl_2$ behave differently under photoionisation conditions using tunable vacuum-UV radiation.

2. Experimental

The apparatus used for the TPEPICO study has been described in detail previously [17]. It consists of a threshold electron detector and a time of flight (TOF) mass spectrometer aligned opposite each other across the interaction region. With suitable electronics it is possible to detect the electrons and ions, generated from a precursor neutral irradiated by vacuum-UV radiation, in coincidence. Such an experiment can determine the fragment ions produced from a defined electronic state of the parent cation and the kinetic energy (KE) release into that ion, from which the dynamics of the fragmentation may be inferred. All measurements were performed using tunable vacuum-UV radiation from the Daresbury synchrotron source and a 5 m focal length, normal-incidence McPherson monochromator, range 8-30 eV (station 3.2).

Three different types of spectra can be recorded. First, the threshold photoelectron (TPES) spectrum can be obtained by recording the threshold electron signal as a function of photon energy. Second, a TPEPICO spectrum can be recorded by collecting the coincidence signal as a function of photon energy. The raw spectrum is a three-dimensional false-colour map of coincidence counts *vs.* TOF *vs.* photon energy. Cuts from the map at fixed ion TOF produce the ion yields as a function of photon energy. Finally, if the photon energy is fixed, higher-resolution TOF spectra can be produced at the optimum time resolution of our apparatus, 8 ns, limited by the time-to-digital converter. Analysis of the peak shape of the TPEPICO-TOF spectrum can reveal the kinetic energy release into the ion, and hence the fraction of energy released into translational motion of the fragments, $\langle f \rangle_t$. Comparison of $\langle f \rangle_t$ to impulsive and statistical models can indicate which mechanism operates. The analysis and models have been discussed in detail in previous papers [18,19]. For a pure impulsive model, $\langle f \rangle_t$ is determined solely by kinematics, being given by μ_b / μ_f where μ_b is the reduced mass of the two atoms whose bond is broken and μ_f is the reduced mass of the two product fragments [20]. Using a statistical model, data are needed for the vibrational frequencies of the fragment ion [21]. If such data is not available, a lower limit for $\langle f \rangle_t$ can be estimated by $1 / (x+1)$ where x is the number of vibrational degrees of freedom in the unimolecular dissociation transition state [22]; for a non-linear molecule such as $C_2H_2Cl_2$, $x = 3N-7$, which gives $x = 11$ when $N = 6$.

3. *Ab initio* calculations

To help interpretation of the data, we calculated the structures and molecular orbitals (MO) of all three isomers of $C_2H_2Cl_2$ using Gaussian 03 [23]. Initially, structures were optimised starting from experimental values given by gas-phase electron diffraction [24,25] and microwave measurements [26] at the MP2 level of theory using a 6-311 G+(d,p) basis set. Optimised structures were very similar to the initially-input experimental structures. We also calculated the ionisation energies of the molecular orbitals using the outer valence Green's function (OVGF) method built into Gaussian 03. Due to the limitations of this method only applying to outer-valence orbitals, Gaussian 03 will only perform this calculation for MOs with energies up to 20 eV. The MP2 and OVGF calculations gave the same relative ordering of orbitals for all isomers of $C_2H_2Cl_2$.

4. Energetics

From the ion yield spectra, we extract appearance energies of the fragment ions at 298 K, AE_{298} (Table 1 Column 2). The AE_{298} values are measured from the first onset of signal above the background noise. At the resolution and step size used, this is equivalent to extrapolation of the linear part of the ion yield to zero

signal, and more sophisticated procedures to fit the threshold region are not necessary. For major ions, defined as fragments formed by breaking a single bond, AE_{298} can converted to an upper limit for $\Delta_r H^0_{298}$, the enthalpy change of the corresponding unimolecular reaction, using the method of Traeger and McLoughlin [27]. This methodology and its limitations when applied to these experiments are discussed elsewhere [4,28]. The upper limit arises due to the possible presence of an exit-channel barrier and/or a kinetic shift; if both are zero, the conversion is exact. This procedure does not apply to the parent ion, strictly only applies for fragmentations involving a single-bond cleavage, and was developed for interpretation of photoionisation yields rather than state-selected TPEPICO yields. Noting these approximations, we have applied this procedure to the $C_2H_2Cl^+ + Cl$ dissociation channel for all three isomers of $C_2H_2Cl_2$, with vibrational frequencies of $C_2H_2Cl^+$ being calculated using Gaussian 03 at the B3LYP 6-311-G+(d,p) level. The results are shown in Column 3 of Table 1. The predicted enthalpies of reaction at 298 K, $\Delta_r H^0_{298,\,calc}$, listed in Column 4 are the sum of the enthalpies of formation of the products minus that of the neutral reactant, using the bracketed values given in kJ mol^{-1} in Column 1. The product enthalpies of formation at 298 K are taken from standard sources [29,30], those of the three isomers of $C_2H_2Cl_2$ from Manion [31], whilst those for the isomers of $C_2H_2Cl^+$ (1040, 1035 and 1033 kJ mol^{-1} for Cl-atom loss from 1,1-, *cis*-1,2- and *trans*-1,2-$C_2H_2Cl_2^+$, respectively) were calculated assuming that the appearance energy of these ions occurs at their thermochemical threshold. These values for $C_2H_2Cl^+$ supercede the slightly higher values given in our earlier paper [2] following a re-analysis of the ion threshold regions. Note also that the two forms of $C_2H_2Cl^+$ following Cl-atom loss from the *cis*-1,2 and *trans*-1,2 isomers of $C_2H_2Cl_2^+$ will be structurally similar if there is free rotation about the carbon-carbon double bond. For the minor ions, defined as those formed by the cleavage of more than one bond, a comparison of AE_{298} for these ions with $\Delta_r H^0_{298,\,calc}$ can indicate the neutral partner(s) that form from photofragmentation of the parent molecule.

5. Results

Figures 1-3 present (a) the threshold photoelectron spectrum and energies of the molecular orbitals calculated by the OVGF method, (b) the ion yield curves, and (c) the branching ratios over the range 10-22 eV for the 1,1, *cis*-1,2 and *trans*-1,2 isomers of dichloroethene, respectively. The spectra were recorded with an optical resolution of 0.3 nm and a TOF resolution of 64 ns, allowing all possible fragment ions to fit onto one 3-D coincidence map. The ionic products observed over this energy range are $C_2H_2Cl_2^+$, $C_2H_2Cl^+$ and $C_2H_2^+$. With a TOF resolution of 64 ns, the loss of one hydrogen atom from any of these three ions would shift the TOF by only one acquisition channel in the TDC. We measured the TPEPICO-TOF spectra with a higher TOF resolution, 8 ns, at the energies of peaks in the threshold photoelectron spectra, but the presence of

$C_2HCl_2^+$, C_2HCl^+ or C_2H^+ was not observed in any isomer. We therefore assume that the H-atom loss channel from any of the three ion products is insignificant, in broad agreement with the interpretation of the electron ionisation data of Momigny [11].

The adiabatic ionisation energies (IE) of the 1,1, *cis*-1,2 and *trans*-1,2 isomers of $C_2H_2Cl_2$ are determined to be 9.78 ± 0.05, 9.62 ± 0.05 and 9.58 ± 0.05 eV, respectively. These data are in good agreement with earlier studies, with the majority reporting a higher value for the IE of the 1,1 isomer. Working under supersonic beam conditions, Woo *et al.* [15] and Bae *et al.* [16] report an adiabatic IE for the *trans*-1,2 isomer of 9.6310 ± 0.0002 and 9.6306 ± 0.0002 eV, respectively. These values are slightly higher than our 298 K value, as expected for a measurement made at a much lower temperature. In C_{2v} symmetry, the outer-valence MOs of the 1,1 isomer of $C_2H_2Cl_2$ are calculated at the MP2 level of theory to be:

..... $(7a_1)^2 (5b_2)^2 (8a_1)^2 (9a_1)^2 (6b_2)^2 (10a_1)^2 (2b_1)^2 (7b_2)^2 (11a_1)^2 (2a_2)^2 (8b_2)^2 (3b_1)^2$.

The corresponding orbitals of *cis*-1,2 $C_2H_2Cl_2$, also in C_{2v} symmetry, are labelled:

…… $(6a_1)^2 (6b_2)^2 (7a_1)^2 (7b_2)^2 (8a_1)^2 (9a_1)^2 (8b_2)^2 (2b_1)^2 (2a_2)^2 (10a_1)^2 (9b_2)^2 (3b_1)^2$

Trans-1,2 $C_2H_2Cl_2$ has C_{2h} symmetry, and the orbitals are labelled:

..... $(6a_g)^2 (6b_u)^2 (7a_g)^2 (7b_u)^2 (8a_g)^2 (8b_u)^2 (9a_g)^2 (2a_u)^2 (2b_g)^2 (9b_u)^2 (10a_g)^2 (3a_u)^2$.

The numbering of the orbitals includes all core orbitals. The symmetries and relative ordering of the orbitals are in excellent agreement with previous calculations of von Niessen *et al.* [7], but only the ordering for the 1,1 isomer agrees with the Hartree-Fock self consistent field (HF-SCF) calculations of Mei *et al.* [12-14]. Using our calculated MP2 geometries, we also performed HF-SCF calculations. These gave the same ordering of the orbitals as the MP2-SCF calculations referred to above. Our small differences from Mei *et al.* therefore appear to arise from the level of theory used to optimise the structures, and not the level of theory used in the SCF calculations.

Table 2 lists experimental vertical ionisation energies (VIE) for the ground and first eight excited states, $\tilde{X}$ - $\tilde{G}$, of the isomers of $C_2H_2Cl_2^+$. For each isomer, the VIEs have been calculated by the OVGF method, these data are also shown in Table 2 together with the pole strengths, and the results are plotted with the TPES in Figs. 1(a)-3(a). The OVGF pole strengths shown in the Figures have been normalized to the height of the first peak in the TPES. The calculated VIEs are in reasonable agreement with experimental values, although there is some evidence that agreement worsens with decreasing electron binding energy. The three isomers

have a similar progression of states whose energies change little between isomers, and our experimental energies are in excellent agreement with those of von Niessen *et al.* [7]. The only significant difference between the isomers is found for the $\tilde{F}$ and $\tilde{G}$ sixth and seventh excited states of the parent ion. For the 1,1 and *trans*-1,2 isomers, these states are very close in energy and form an unresolved peak in the TPES; the peak in the *trans*-1,2 isomer is significantly narrower, as predicted by the OVGF calculations. For the *cis*-1,2 isomer, the states have a much greater energy gap and are well resolved. This difference can be explained by symmetry arguments. In the *cis*-1,2 isomer, both the $\tilde{F}$ and $\tilde{G}$ states have $^2A_1$ symmetry, and the states may interact with each other to a significant extent and become separated in energy. For the 1,1 and *trans*-1,2 isomers, these two states have different symmetries, and therefore there is no such interaction. An alternative explanation can be offered from a description of the nature of these orbitals. For all three isomers, the atomic orbitals which contribute to the MOs are similar. However, for the $\tilde{G}\ ^2A_1$ state of the *cis*-1,2 isomer there is extensive delocalisation of electron density which is not present for this state of the other isomers. This difference in bonding may cause a separation in the energies of the $\tilde{F}$ and $\tilde{G}$ states for this isomer of $C_2H_2Cl_2^+$.

The ion yields and breakdown diagrams show similar behaviour for the three isomers (Figs. 1-3, (b) and (c)). The ground, $\tilde{X}$, and first excited state, $\tilde{A}$, of all isomers are stable with respect to fragmentation, and the parent ion is the only species observed from onset of ionisation to *ca.* 12 eV. The parent ion yield and the TPES therefore mimic each other. In the range 12-17 eV, encompassing the $\tilde{B}$ through $\tilde{G}$ states of the parent ion, Cl-atom loss dominates, and the ion yield of $C_2H_2Cl^+$ now mimics the TPES. The $AE_{298}(C_2H_2Cl^+)$ values from the 1,1, *cis*-1,2 and *trans*-1,2 isomers of $C_2H_2Cl_2$ are 11.88 ± 0.05, 11.88 ± 0.05 and 11.84 ± 0.05 eV, respectively. For energies above 16 eV, $C_2H_2^+$ signal is observed, and becomes the dominant product ion for hν > 17 eV. Table 1 lists the fragment ions and their respective AE_{298} values. As mentioned in Section 4, since the production of $C_2H_2Cl^+$ from $C_2H_2Cl_2^+$ involves a simple C-Cl bond cleavage, it is assumed that there will be no exit-channel barrier in this reaction, and therefore that $C_2H_2Cl^+$ turns on at its thermochemical threshold. Values for $\Delta_fH^o_{298}(C_2H_2Cl^+)$ thus derived using the procedure of Traeger and McLoughlin [27] were given in Section 4. The onsets for formation of $C_2H_2^+$ (16.28 ± 0.15, 16.47 ± 0.15 and 16.28 ± 0.15 eV for the 1,1, *cis*-1,2 and *trans*-1,2 isomers of $C_2H_2Cl_2$, respectively) lie very close to the thermochemical threshold if two Cl atoms form with this ion, but *ca.* 2.5 eV above threshold if Cl_2 is the neutral partner. Formation of Cl_2 is almost certain to involve an exit-channel barrier, so the experimental energetics cannot rule out this possibility. Whilst formation of a Cl-Cl bond is easy to imagine following dissociation of the 1,1 and *cis*-1,2 isomers, the transition state from the *trans*-1,2 isomer is likely to be highly constrained, and this step seems very unlikely to occur. The consistency of the onset for all three

isomers of $C_2H_2Cl_2$ suggests the same mechanism is occurring. The former reaction is therefore more likely, and the data suggest strongly that $C_2H_2^+$ forms *via* secondary dissociation of $C_2H_2Cl^+$. Finally, we note that the isomeric effect observed in the threshold photoelectron spectra between 16-17 eV is not observed in the ion yields and breakdown diagram over this range.

TPEPICO-TOF spectra in the non-scanning mode have been recorded at high resolution, 8 ns, at the energies of the peaks in the threshold photoelectron spectra. The parent ion TOF spectra show the expected convolution of three Gaussian distributions centred on TOFs corresponding to ions with *m/e* values of 96, 98 and 100 with weightings of 9:6:1; see ref. [18] for an example of such a fit. TPEPICO-TOF spectra of the $C_2H_2Cl^+$ daughter ion have been analysed in the normal way, yielding the kinetic energy release distribution (KERD) and hence the total average kinetic energy release, $<KE>_t$ (Table 3, Column 6) [32]. Briefly, for each spectrum a small basis set of peaks, each with a discrete energy release ε_t is computed, and assigned a probability. The discrete energies are given by $\varepsilon_t(n) = (2n-1)^2\Delta E$, where n = 1,2,3,4 ….. ΔE depends on the statistical quality of the data ; the higher the signal-to-noise ratio, the lower ΔE and the higher n can be set. Each computed peak in the kinetic energy release distribution spans the range $4(n-1)^2\Delta E$ to $4n^2\Delta E$, centred at $\varepsilon_t(n) + \Delta E$. The reduced probability of each discrete energy, $P(\varepsilon_t)$, is varied by linear regression to minimise the least-squared errors between the simulated and experimental TOF peak. From the basis set of ε_t and $P(\varepsilon_t)$, $<KE>_t$ is easily determined. Thus Fig. 4(a) shows a spectrum of $C_2H_2Cl^+$ formed from dissociative photoionisation of *trans*-1,2-$C_2H_2Cl_2$ at 12.77 eV, the peak of the $\widetilde{C}\ ^2B_g$ state of the parent ion, and Fig. 4(b) shows the KERD from which a $<KE>_t$ value of 0.36 ± 0.03 eV is determined. The analysis can account for isotopomers in the daughter ion [32], and allowance is made for that component of the peak broadening caused by the presence of two Cl isotopes in $C_2H_2Cl^+$.

By comparing such $<KE>_t$ values with the available energy, the fractional release into translational energy of $C_2H_2Cl^+ + Cl$, $<f>_t$ (expt) is determined (Table 3, Column 7). These values for $<f>_t$ can be compared with the predictions of statistical and pure-impulsive models [20-22] (Table 3, Columns 8 and 9). For all three isomers, the value of $<f>_t$ decreases with increasing energy. For dissociation of the $\widetilde{B}$ state of $C_2H_2Cl_2^+$, the value of $<f>_t$, 0.32-0.36, is very close to the pure-impulsive value of 0.40, whereas dissociation of higher-lying valence states leads to $<f>_t$ values less than 0.10 and much closer to the statistical value of 0.08. This behaviour has been observed in previous studies by our group for similar-sized molecules [34], and is characteristic of behaviour based on the theories of intramolecular vibrational energy redistribution. That is, as the photon energy increases, successively more electronic and vibrational states of the parent ion can be accessed, so there is less chance of fragmentation occurring along a specific potential energy surface *via* a

selective C–Cl bond dissociation. Energy randomisation within the molecule is more likely to occur, leading to a lower value of $\langle f \rangle_t$.

In studies of the reactions of small cations and anions with $C_2H_2Cl_2$ [2,5], we investigated the effects of the isomeric form of $C_2H_2Cl_2$ on rate coefficients and product branching ratios. In the cation study, very significant isomeric effects were observed with CF^+ and CF_3^+ where the recombination energy (RE) of the ion is less than the IE ($C_2H_2Cl_2$); for example, the only product from the reaction of CF_3^+ with 1,1-$C_2H_2Cl_2$ is $C_2H_2Cl^+$, whereas the reaction with either 1,2 isomer only produces $CHCl_2^+$ [2]. Energetically, such reactions cannot proceed by charge transfer, but can only occur through the formation of a chemical complex in which new bonds are formed and broken, where isomeric (and steric) effects might be expected to be important. For the reactions of cations with RE values greater than the IE ($C_2H_2Cl_2$), the differences between the three isomers are less significant, but small effects (*i.e.* product branching ratios which differ outside experimental error) are observed for the reactions of SF^+, CO_2^+, CO^+, N_2^+ and Ar^+ whose RE values span 10.3-15.8 eV. Within the accuracy of our determination of product branching ratios, isomeric effects are insignificant for the reactions of atomic ions Kr^+ (RE = 14.00 eV), F^+ (17.42 eV) and Ne^+ (21.56 eV), and the product branching ratios are similar to those from this TPEPICO study. These reactions therefore probably proceed by long-range charge transfer [3,4]. We note that the atomic ion which shows anomalous behaviour, Ar^+, has an RE value, 15.76 eV, which is close to the energy of the $\tilde{F}$ and $\tilde{G}$ states of $C_2H_2Cl_2^+$ where the clearest isomeric differences are observed in the threshold photoelectron spectra. The TPEPICO results show that any isomeric effects following dissociative photoionisation are small, with the only clear difference being the behaviour of the $\tilde{F}$ and $\tilde{G}$ states of the parent ion in the range 15.7-17.0 eV. We were unable to examine this range in the cation-molecule study in detail because a number of cations with suitable RE values were not readily available, thus it was not possible to see if subtle differences in the TPEPICO study were mirrored in the complementary study.

6. Conclusions

We have studied the photoionisation dynamics of the three isomers of $C_2H_2Cl_2$ using synchrotron radiation in the photon energy range 9–23 eV by threshold photoelectron photoion coincidence spectroscopy. The energies of the electronic states of the parent ion are in excellent agreement with outer valence Green function calculations of the energies of the molecular orbitals of $C_2H_2Cl_2$. New upper limits have been determined for the enthalpy of formation at 298 K of $C_2H_2Cl_2^+$ and $C_2H_2Cl^+$ for all isomers. The only clearly observable isomeric effect in photoionisation of $C_2H_2Cl_2$ is a separation of the $\tilde{F}\ ^2A_1$ and $\tilde{G}\ ^2A_1$ states of

$C_2H_2Cl_2^+$ for the *cis*-1,2 isomer. Isomeric effects have been observed in the reactions of small cations and anions with $C_2H_2Cl_2$ [2,5], but they appear to show little relationship to this effect observed in photoionisation. Thus, the reactions of CF^+ and CF_3^+ yield completely different products for the 1,1 and 1,2 isomers. The reactions of small anions (*e.g.* O^-, O_2^-, OH^-, F^- and CF_3^-) yield $C_2HCl_2^-$ as the major product from the *trans*-1,2 isomer, whilst this product is not observed from the 1,1 and *cis*-1,2 isomers. This is the only example of significantly different behaviour of the *cis*- and *trans*-1,2 isomers.

The translational kinetic energy released into $C_2H_2Cl^+ + Cl$ at the energies of the peaks in the threshold photoelectron spectra has been determined for the three isomers. For low-lying excited states of $C_2H_2Cl_2^+$, the fractional energy release has values characteristic of impulsive dissociation, suggesting that these states display isolated-state behaviour and dissociate along specific potential energy pathways. For higher-lying excited valence states of $C_2H_2Cl_2^+$, the $\langle f \rangle_t$ values reduce to that characteristic of statistical behaviour. Now, energy is randomised rapidly in the initially-populated state of $C_2H_2Cl_2^+$, internal conversion occurs to the ground state and dissociation takes place from that surface with a smaller fraction of the available energy channelled into translational energy of the two products

Acknowledgments

We are grateful to EPSRC for grants (GR/M42974 and GR/S21557) and useful discussions with Dr Victor Mikhailov. MAP, SA and CRH thank the University of Birmingham, *via* the EPSRC Doctoral Training Account, for research studentships.

References

[1] T. Yamada, A. el-Sinawi, M. Siraj, P.H. Taylor, J. Peng, X. Hu, P. Marshall, *J. Phys. Chem. A.*, **105**, 7588 (2001).

[2] V.A. Mikhailov, M.A. Parkes. R.P. Tuckett, C.A. Mayhew, *J. Phys. Chem. A.,* **110**, 5760 (2006).

[3] G. K. Jarvis, R. A. Kennedy, C. A. Mayhew and R. P. Tuckett, *Int. J. Mass Spectrom.,* **202**, 323 (2000).

[4] M. A. Parkes, S. Ali, R. P. Tuckett, V. A. Mikhailov, C. A. Mayhew, *Phys. Chem. Chem. Phys*., **8**, 3643 (2006).

[5] R.A. Kennedy, C.A. Mayhew, R. Peverall, P. Watts, *Phys. Chem. Chem. Phys.,* **2**, 3145 (2000).

[6] R.F. Lake, H. Thompson, *Proc. Roy. Soc. (London) A.,* **315**, 323 (1970).

[7] W. von Niessen, L. Åsbrink, G. Bieri, *J. Elec. Spec. Rel. Phen.,* **26**, 173 (1982).

[8] K. Wittel, H. Bock, *Chem. Ber.,* **107**, 317 (1974).

[9] N. Jonathan, K. Ross, V. Tomlinson, *Int. J. Mass Spectrom. Ion Phys.,* **4**, 51 (1970).

[10] K. Watanbe, T. Nakayama, J. Mottl, *J. Quant. Spectrosc. Radiat. Transfer,* **2**, 369 (1962).

[11] J. Momigny, *Bull. Soc. Chim. Belg.,* **70**, 241 (1961).

[12] L. Mei, M. Chuaqui, C.P. Mathers, J.F. Ying, K.T. Leung, *Chem. Phys.,* **188**, 347 (1994).

[13] L. Mei, M. Chuaqui, C.P. Mathers, J.F. Ying, K.T. Leung, *J. Chem. Phys.,* **101**, 3558 (1994).

[14] M.H. Chuaqui, L. Mei, C.P. Mathers, M.L. Allison, J.F. Ying, K.T. Leung, *J. Chem. Phys.,* **102**, 90 (1995).

[15] H.K. Woo, P. Wang, K.C. Lau, X. Xing, C.Y. Ng, *J. Phys. Chem. A.,* **108**, 9637 (2004).

[16] Y. J. Bae, M. Lee, M. S. Kim, *J. Phys. Chem. A.,* **110**, 8535 (2006).

[17] P.A. Hatherly, D.M. Smith, R.P. Tuckett, *Zeit. Phys. Chem.,* **195**, 97 (1996).

[18] C.R. Howle, D.J. Collins, R.P. Tuckett, A.E.R. Malins, *Phys. Chem. Chem. Phys.,* **7**, 2287 (2005).

[19] M.A. Parkes, R.Y.L. Chim, C.A. Mayhew, V.A. Mikhailov, R. P. Tuckett, *Mol. Phys.,* **104**, 263 (2006).

[20] K.E. Holdy, L.C. Klots, K.R. Wilson, *J. Chem. Phys.,* **52**, 4588 (1970).

[21] C.E. Klots, *J. Chem. Phys.,* **58**, 5364 (1973).

[22] J.L. Franklin, *Science,* **193**, 725 (1976).

[23] Gaussian 03, Revision C.02, M. J. Frisch, G. W. Trucks, H. B. Schlegel, G. E. Scuseria, M. A. Robb, J. R. Cheeseman, J. A. Montgomery, Jr., T. Vreven, K. N. Kudin, J. C. Burant, J. M. Millam, S. S. Iyengar, J. Tomasi, V. Barone, B. Mennucci, M. Cossi, G. Scalmani, N. Rega, G. A. Petersson, H. Nakatsuji, M. Hada, M. Ehara, K. Toyota, R. Fukuda, J. Hasegawa, M. Ishida, T. Nakajima, Y. Honda, O. Kitao, H. Nakai, M. Klene, X. Li, J. E. Knox, H. P. Hratchian, J. B. Cross, V. Bakken, C. Adamo, J. Jaramillo, R. Gomperts, R. E. Stratmann, O. Yazyev, A. J. Austin, R. Cammi, C. Pomelli, J. W. Ochterski, P. Y. Ayala, K. Morokuma, G. A. Voth, P. Salvador, J. J. Dannenberg, V. G. Zakrzewski, S. Dapprich, A. D. Daniels, M. C. Strain, O. Farkas, D. K. Malick, A. D. Rabuck, K. Raghavachari, J. B. Foresman, J. V. Ortiz, Q. Cui, A. G. Baboul, S. Clifford, J. Cioslowski, B. B. Stefanov, G. Liu, A. Liashenko, P. Piskorz, I. Komaromi, R. L. Martin, D. J. Fox, T. Keith, M. A. Al-Laham, C. Y. Peng, A. Nanayakkara, M. Challacombe, P. M. W. Gill, B. Johnson, W. Chen, M. W. Wong, C. Gonzalez, and J. A. Pople, Gaussian, Inc., Wallingford CT, 2004.

[24] M. I. Davies, H. P. Hanson, *J. Phys. Chem.,* **69**, 4091 (1965).

[25] L. Schäfer, J. D. Ewbank, K. Siam, D. W. Paul, D. L. Monts, *J. Mol. Struct.,* **145**, 135 (1986).

[26] S. Sekino, T. Nishikawa, *J. Phys. Soc. Jpn.,* **12**, 43 (1957).

[27] J. C. Traeger, R. G. McLoughlin, *J. Am. Chem. Soc.,* **103**, 3647 (1981).

[28] W. Zhou, D. J. Collins, R. Y. L. Chim, D. P. Seccombe, R. P. Tuckett, *Phys. Chem. Chem. Phys.,* **6**, 3081 (2004).

[29] M. W. Chase, *J. Phys. Chem. Ref. Data,* monograph no. 9 (1998).

[30] S. G. Lias, J. E. Bartmess, J. F. Lebman, J. L. Holmes, R. D. Levin, W. G. Mallard, *J. Phys. Chem. Ref. Data,* **17**, supplement no 1 (1988).

[31] J. A. Manion, *J. Phys. Chem. Ref. Data,* **31**, 123 (2002).

[32] G.K. Jarvis, D.P. Seccombe, R.P. Tuckett, *Chem. Phys. Letts.,* **315**, 287 (1999).

[33] T. Shimanouchi, "Tables of Molecular Vibrational Frequencies, volume 1", National Bureau of Standards, NSRDS-NBS 39 (1972).

[34] *e.g.* D. P. Seccombe, R. P. Tuckett, B. O. Fisher, *J. Chem. Phys.,* **114**, 4074 (2001).

Table 1. Energetics of the dissociative ionisation pathways of isomers of $C_2H_2Cl_2$.

	AE_{298} [a] / eV	$\Delta_r H^0_{298,\,exp}$ [b] / eV	$\Delta_r H^0_{298,\,calc}$ [c] / eV
Major [d] products of 1,1-$C_2H_2Cl_2$ (2) [e]			
$C_2H_2Cl_2^+$ (946) [g] + e^-	9.78	-	9.78
$C_2H_2Cl^+$ (1040) [h] + Cl (121) + e^-	11.88	12.01	12.01
Minor [f] products of 1,1-$C_2H_2Cl_2$ (2)			
$C_2H_2^+$ (1327) + Cl (121) + Cl (121) + e^-	16.28	-	16.24
$C_2H_2^+$ (1327) + Cl_2 (0) + e^-		-	13.73
Major products of *cis*-1,2-$C_2H_2Cl_2$ (-3)			
$C_2H_2Cl_2^+$ (925) [g] + e^-	9.62	-	9.62
$C_2H_2Cl^+$ (1035) [h] + Cl (121) + e^-	11.88	12.01	12.01
Minor products of *cis*-1,2-$C_2H_2Cl_2$ (-3)			
$C_2H_2^+$ (1327) + Cl (121) + Cl (121) + e^-	16.47	-	16.29
$C_2H_2^+$ (1327) + Cl_2 (0) + e^-		-	13.78
Major products of *trans*-1,2-$C_2H_2Cl_2$ (-1)			
$C_2H_2Cl_2^+$ (923) [g] + e^-	9.58	-	9.58
$C_2H_2Cl^+$ (1033) [h] + Cl (121) + e^-	11.84	11.97	11.97
Minor products of *trans*-1,2-$C_2H_2Cl_2$ (-1)			
$C_2H_2^+$ (1327) + Cl (121) + Cl (121) + e^-	16.28	-	16.27
$C_2H_2^+$ (1327) + Cl_2 (0) + e^-		-	13.76

[a] Experimentally derived appearance energies, measured from onset of signal above noise.
[b] Experimentally measured enthalpy of reaction, derived using the method of Traeger and McLoughlin [27].
[c] Calculated value for enthalpy of reaction given by enthalpy of formation of products minus that of reactants.
[d] Major products are defined as fragments caused by breaking of a single bond.
[e] Literature values for $\Delta_f H^0_{298}$ are given in kJ mol^{-1} in brackets in column 1.
[f] Minor products are defined as fragments formed by breaking of more than one bond.
[g] Calculated heat of formation from $\Delta_f H^0_{298}$ for the neutral plus the appropriate measured ionisation energy.
[h] Calculated from experimental $\Delta_r H^0_{298}$ using Hess' cycle $C_2H_2Cl_2 \rightarrow C_2H_2Cl^+ + Cl + e^-$.

Table 2. Vertical ionisation energies for the three isomers of dichloroethene, $C_2H_2Cl_2$.

	1,1-dichloroethene		*cis*-1,2-dichloroethene		*trans*-1,2-dichloroethene	
State	VIE [a] / eV	OVGF [b] / eV	VIE [a] / eV	OVGF [b] / eV	VIE [a] / eV	OVGF [b] / eV
$\widetilde{X}$	9.89	9.69 (0.91)	10.03	9.45 (0.91)	10.21	9.44 (0.91)
$\widetilde{A}$	11.68	11.41 (0.91)	11.88	11.50 (0.91)	11.88	11.65 (0.91)
$\widetilde{B}$	12.22	11.94 (0.91)	12.08	11.78 (0.91)	12.08	11.81 (0.91)
$\widetilde{C}$	12.55	12.32 (0.91)	12.55	12.31 (0.91)	12.77	12.48 (0.91)
$\widetilde{D}$	13.91	13.89 (0.91)	13.91	13.71 (0.89)	13.91	13.77 (0.90)
$\widetilde{E}$	14.19	14.20 (0.90)	14.19	14.02 (0.91)	14.01	13.94 (0.91)
$\widetilde{F}$	16.15	15.95 (0.90)	15.73	15.55 (0.89)	16.28	16.38 (0.88)
$\widetilde{G}$	16.15	16.58 (0.87)	16.93	17.12 (0.88)	16.28	16.21 (0.89)
$\widetilde{H}$	18.49	18.93 (0.86)	18.90	*c*	18.99	*C*

[a] Vertical ionisation energies, this work.

[b] Calculated vertical ionisation energies using the outer valence Greens' functions method within Gaussian 03 [23]. The pole strength is shown in brackets.

[c] OVGF energies are not calculated above a threshold value of 20 eV in Gaussian 03 [23].

Table 3. Total mean kinetic energy releases, $\langle KE \rangle_t$, for the two-body fragmentation of valence states of isomers of $C_2H_2Cl_2^+$.

Parent Ion	State	Daughter Ion	hν / eV	E_{avail} [a] / eV	$\langle KE \rangle_t$ / eV	$\langle f \rangle_t$ experimental [b]	$\langle f \rangle_t$ statistical	$\langle f \rangle_t$ impulsive
1,1-$C_2H_2Cl_2^+$	$\tilde{B}$	$C_2H_2Cl^+$	12.25	0.45	0.16	0.36	0.08	0.40
	$\tilde{C}$		12.59	0.79	0.24	0.30	0.08	0.40
	$\tilde{D}$ / $\tilde{E}$		14.19	2.39	0.60	0.25	0.08	0.40
	$\tilde{F}$ / $\tilde{G}$		16.21	4.41	0.77	0.17	0.08	0.40
	$\tilde{H}$		18.51	6.71	0.53	0.08	0.08	0.40
cis-1,2-$C_2H_2Cl_2^+$	$\tilde{B}$	$C_2H_2Cl^+$	12.55	0.75	0.24	0.32	0.08	0.40
	$\tilde{D}$ / $\tilde{E}$		14.19	2.39	0.54	0.23	0.08	0.40
	$\tilde{F}$		15.73	3.93	0.58	0.15	0.08	0.40
	$\tilde{G}$		16.73	4.93	0.93	0.19	0.08	0.40
	$\tilde{H}$		18.90	7.10	0.49	0.07	0.08	0.40
trans-1,2-$C_2H_2Cl_2^+$	$\tilde{C}$	$C_2H_2Cl^+$	12.77	1.01	0.36	0.36	0.08	0.40
	$\tilde{D}$ / $\tilde{E}$		14.00	2.24	0.40	0.18	0.08	0.40
	$\tilde{F}$ / $\tilde{G}$		16.28	4.52	0.65	0.14	0.08	0.40
	$\tilde{H}$		19.34	7.58	0.53	0.07	0.08	0.40

[a] E_{avail} = hυ + thermal energy of parent molecule at 298 K (0.08 eV) − $AE_{298,calc}$. Vibrational frequencies of $C_2H_2Cl_2$ from [33]. See text.

[b] Given by $\langle KE \rangle_t$ / E_{avail}.

Figure Captions

Figure 1. (a) Threshold photoelectron spectrum and calculated OVGF spectrum, (b) ion yields, (c) breakdown diagram for 1,1-dichloroethene over the energy range 10-22 eV. The photon resolution is 0.3 nm.

Figure 2. (a) Threshold photoelectron spectrum and calculated OVGF spectrum, (b) ion yields, (c) breakdown diagram for *cis*-1,2-dichloroethene over the energy range 10-22 eV. The photon resolution is 0.3 nm.

Figure 3. (a) Threshold photoelectron spectrum and calculated OVGF spectrum, (b) ion yields, (c) breakdown diagram for *trans*-1,2-dichloroethene over the energy range 10-22 eV. The photon resolution is 0.3 nm.

Figure 4. (a) Coincidence TOF spectrum of $C_2H_2Cl^+$ photoionised at 12.77 eV into the $\widetilde{C}\ ^2B_g$ state of the parent ion of *trans*-1,2-$C_2H_2Cl_2$ (black dots). The solid line is the best fit to the data, comprised of three contributions with ε_t = 0.04, 0.36 and 1.00 eV (coloured lines). The reduced probability of each contribution is shown in (b). The fit yields a total mean translational kinetic energy, $\langle KE \rangle_t$, into $C_2H_2Cl^+ + Cl$ of 0.36 ± 0.03 eV.

Figure 1

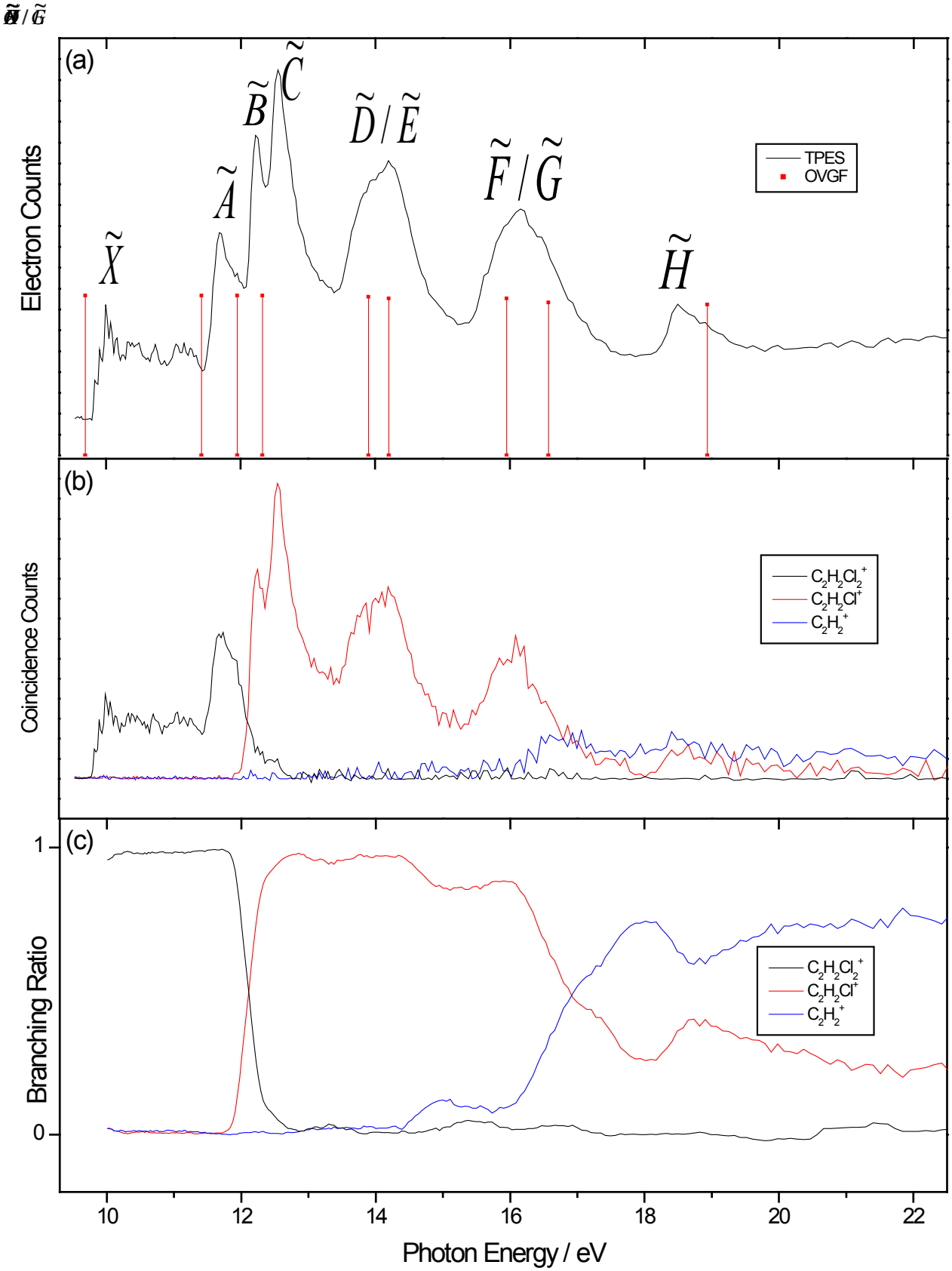
(a)
$\tilde{X}$
$\tilde{A}$
$\tilde{B}$
$\tilde{C}$
$\tilde{D}/\tilde{E}$
$\tilde{F}/\tilde{G}$
$\tilde{H}$
TPES
OVGF
Electron Counts
(b)
$C_2H_2Cl_2^+$
$C_2H_2Cl^+$
$C_2H_2^+$
Coincidence Counts
(c)
1
0
Branching Ratio
10
12
14
16
18
20
22
Photon Energy / eV

Figure 2

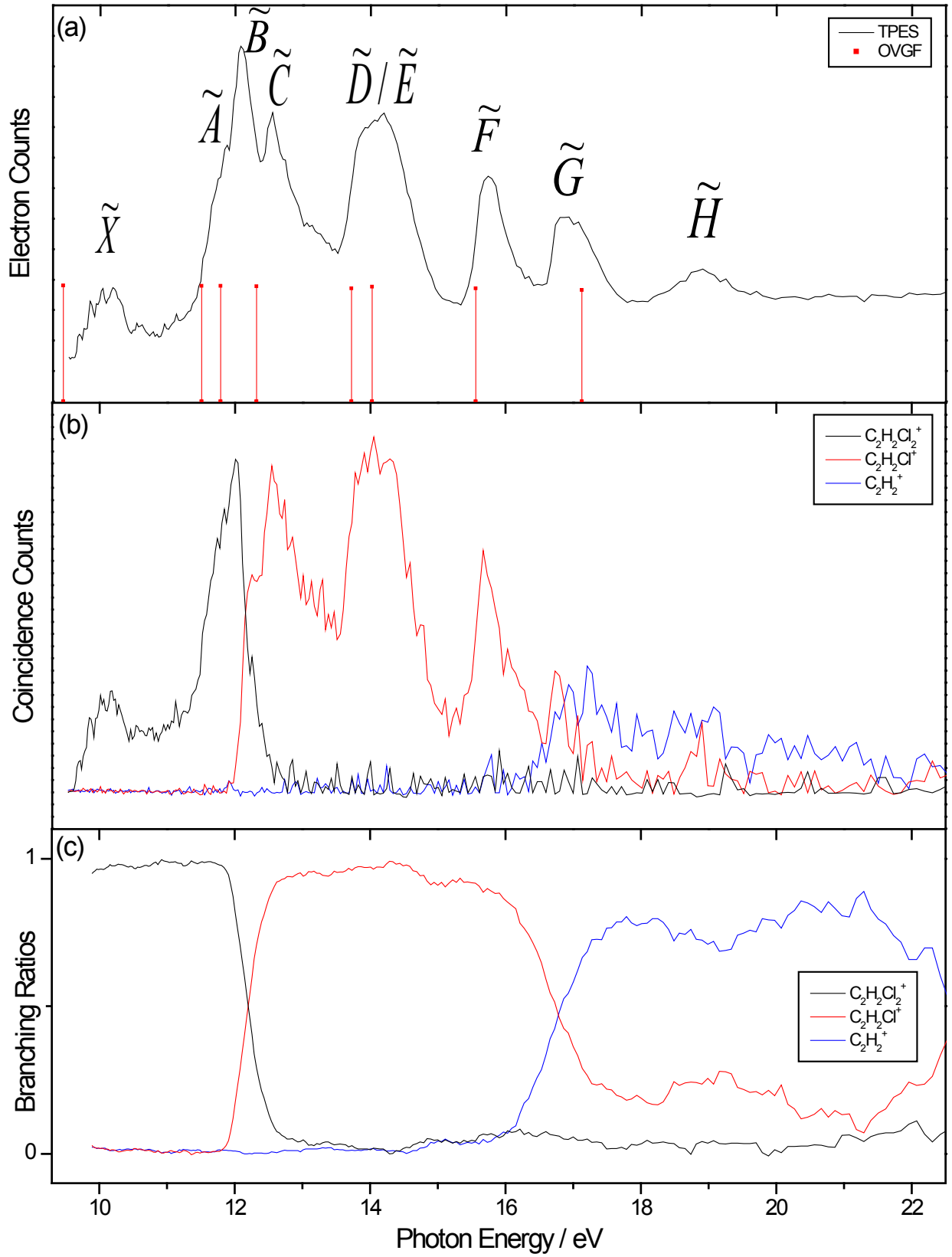
(a)
TPES
OVGF
Electron Counts
$\tilde{X}$
$\tilde{A}$
$\tilde{B}$
$\tilde{C}$
$\tilde{D}/\tilde{E}$
$\tilde{F}$
$\tilde{G}$
$\tilde{H}$
(b)
$C_2H_2Cl_2^+$
$C_2H_2Cl^+$
$C_2H_2^+$
Coincidence Counts
(c)
Branching Ratios
1
0
10
12
14
16
18
20
22
Photon Energy / eV

Figure 3

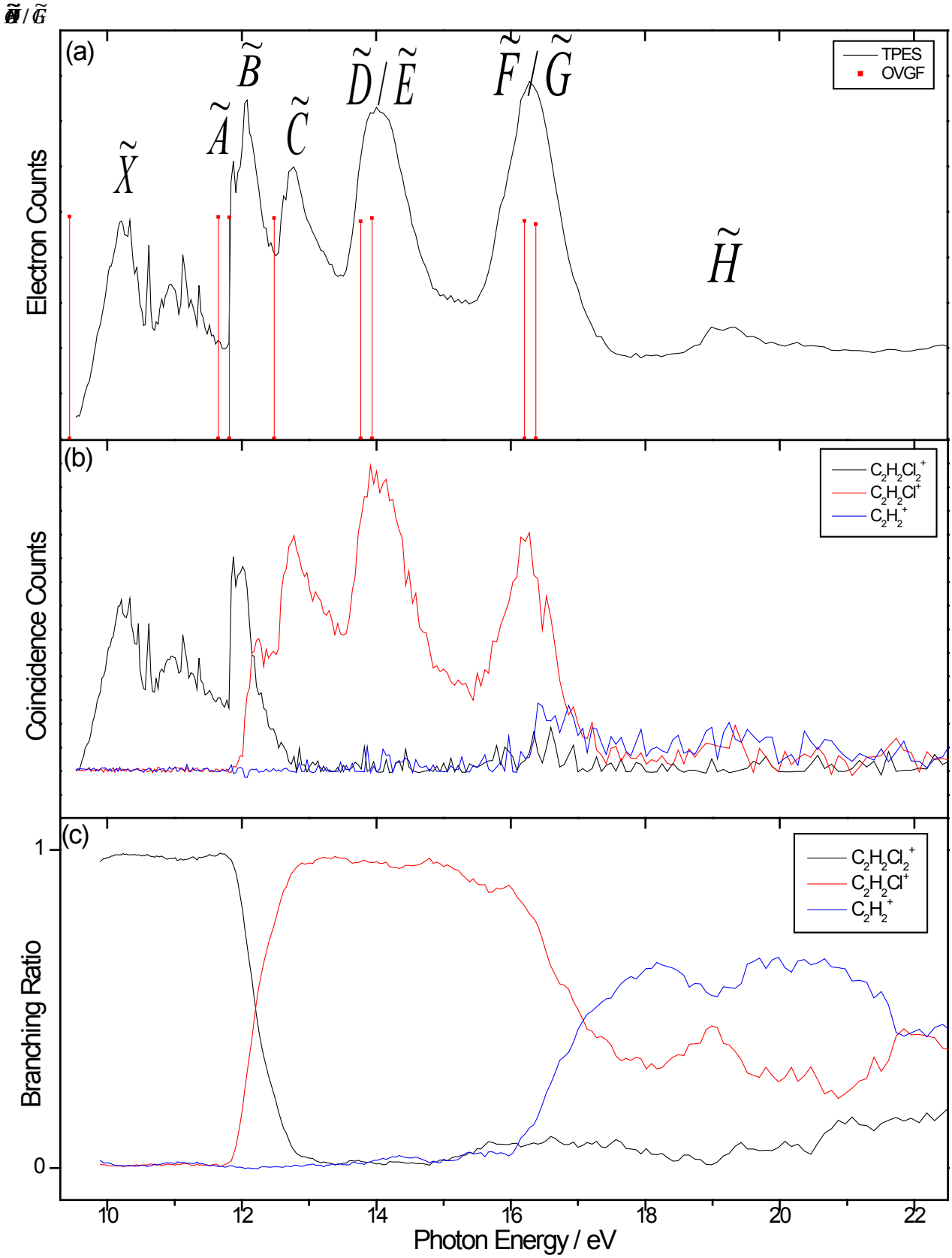
(a)
TPES
OVGF
Electron Counts
$\tilde{X}$
$\tilde{A}$
$\tilde{B}$
$\tilde{C}$
$\tilde{D}/\tilde{E}$
$\tilde{F}/\tilde{G}$
$\tilde{H}$
(b)
$C_2H_2Cl_2^+$
$C_2H_2Cl^+$
$C_2H_2^+$
Coincidence Counts
(c)
$C_2H_2Cl_2^+$
$C_2H_2Cl^+$
$C_2H_2^+$
Branching Ratio
1
0
10
12
14
16
18
20
22
Photon Energy / eV

Figure 4

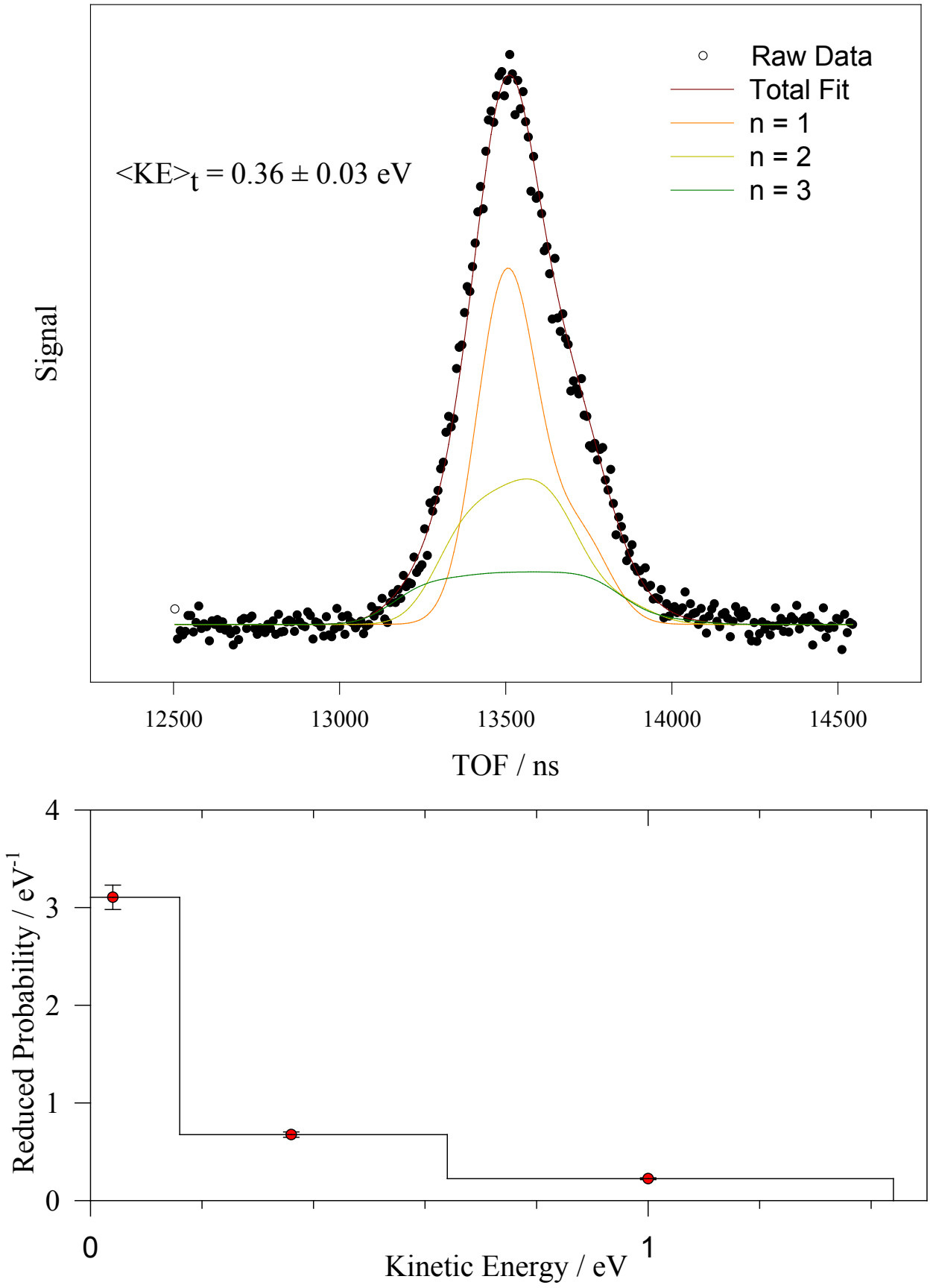
Raw Data
Total Fit
n = 1
n = 2
n = 3
<KE>t = 0.36 ± 0.03 eV
Signal
12500
13000
13500
14000
14500
TOF / ns
4
3
2
1
0
Reduced Probability / eV-1
0
1
Kinetic Energy / eV